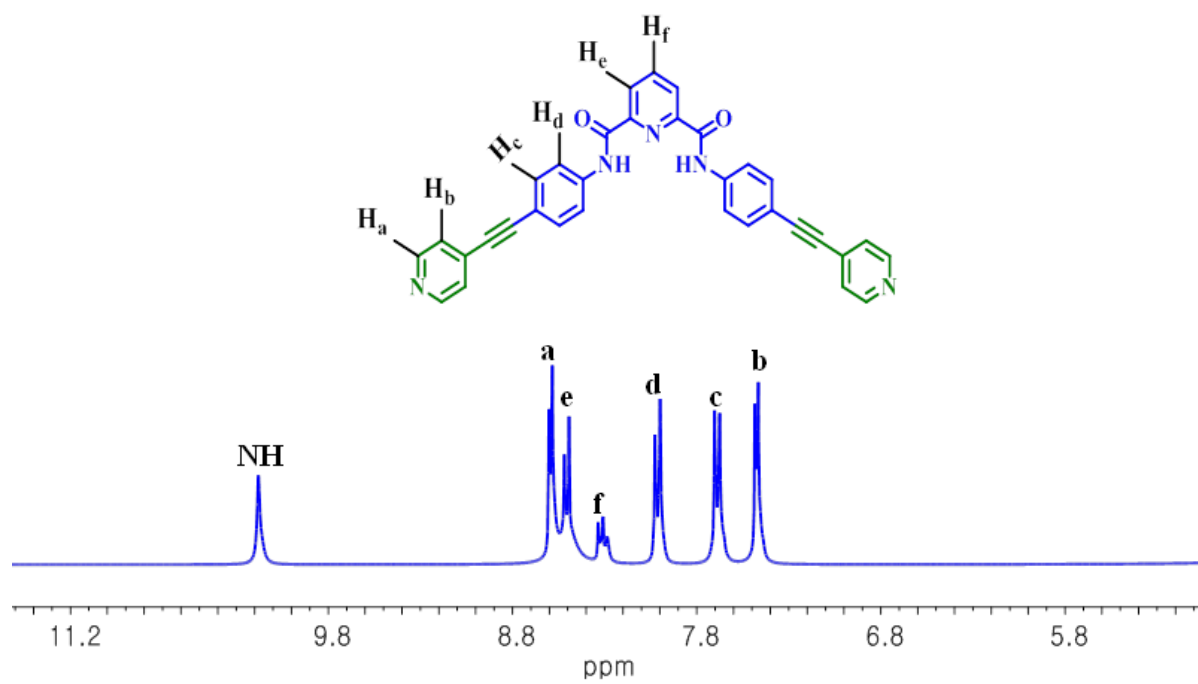


Electronic Supporting Information

For the

**New arene-Ru based supramolecular coordination complex for efficient binding and selective sensing of green fluorescent protein**

Anurag Mishra,<sup>a,‡</sup> Sambandam Ravikumar,<sup>b,f,‡</sup> Young Ho Song,<sup>a</sup> Nadarajan Saravanan Prabhu,<sup>c</sup> Hyunuk Kim,<sup>d,\*</sup> Soon Ho Hong,<sup>b</sup> Seyeon Cheon,<sup>e</sup> Jaegeun Noh,<sup>e</sup> and Ki-Whan Chi<sup>a,\*</sup>



**Figure S1.**  $^1\text{H}$  NMR of ligand **1** in Nitromethane- $d_3$

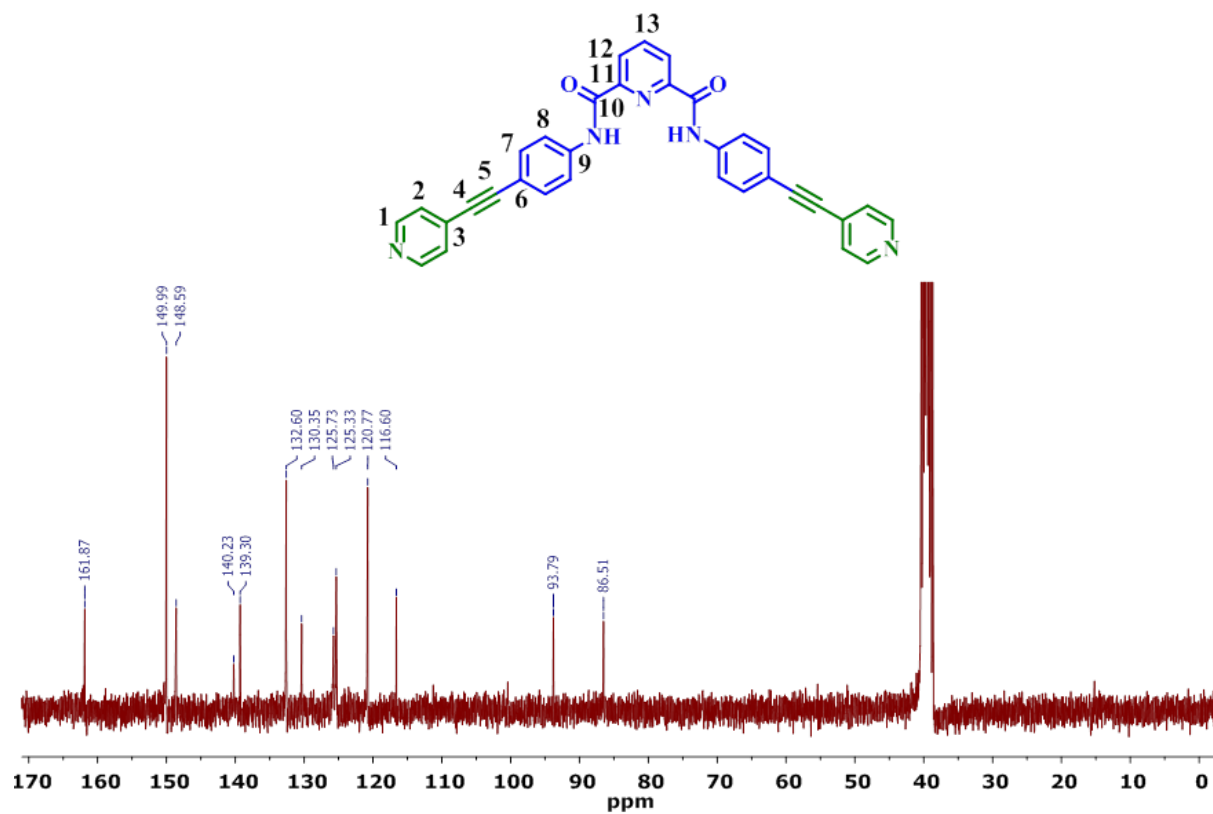


**Figure S2.**  $^{13}\text{C}$  NMR of ligand **1** in  $\text{DMSO-d}_6$

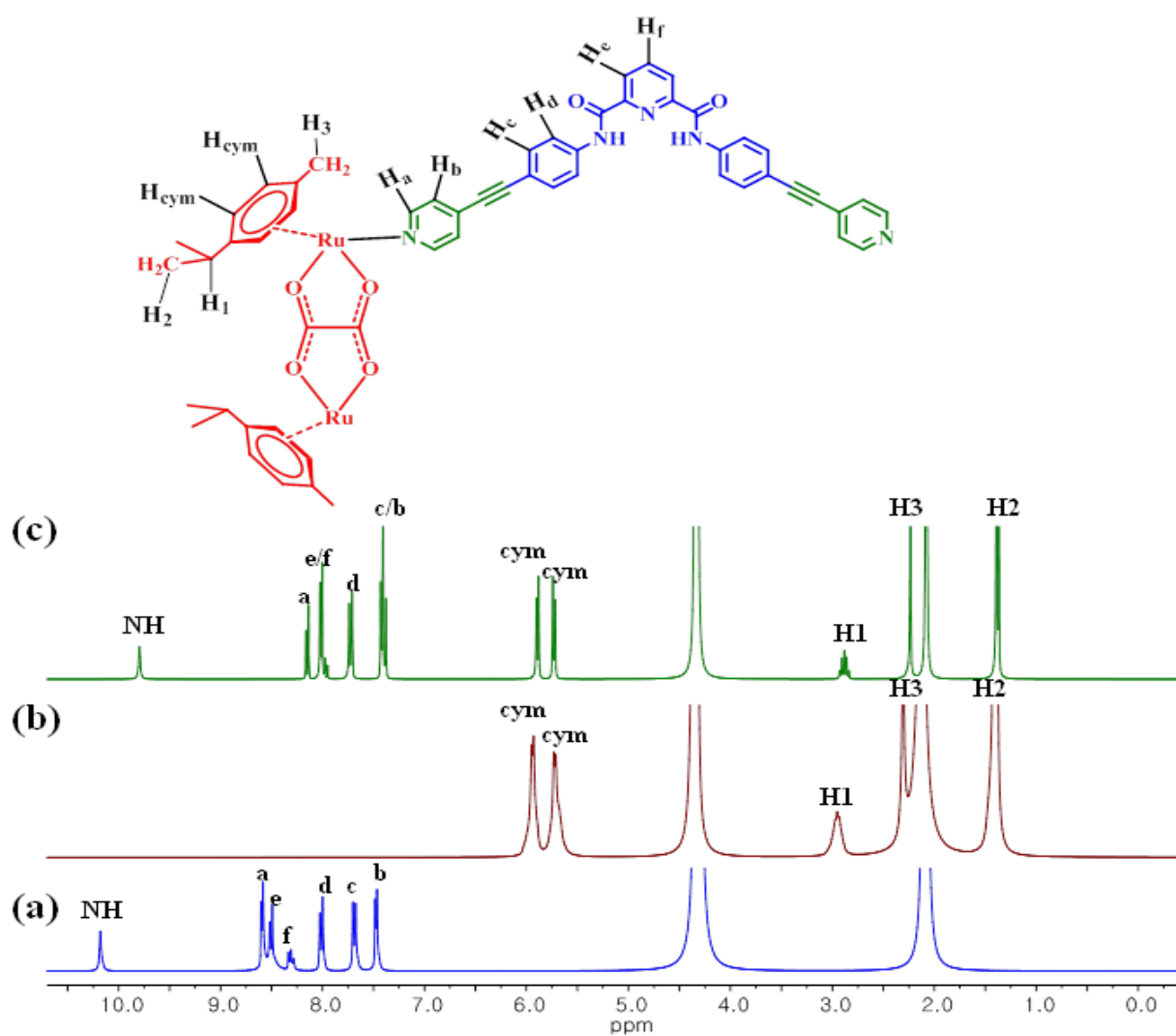


**Figure S3.** Comparison between the aromatic region of the  $^1\text{H}$  NMR spectra of (a) ligand **1** (b) Ru acceptor **2** (c) the [2 + 2] self-assembly **3**, all in Nitromethane- $\text{d}_3$

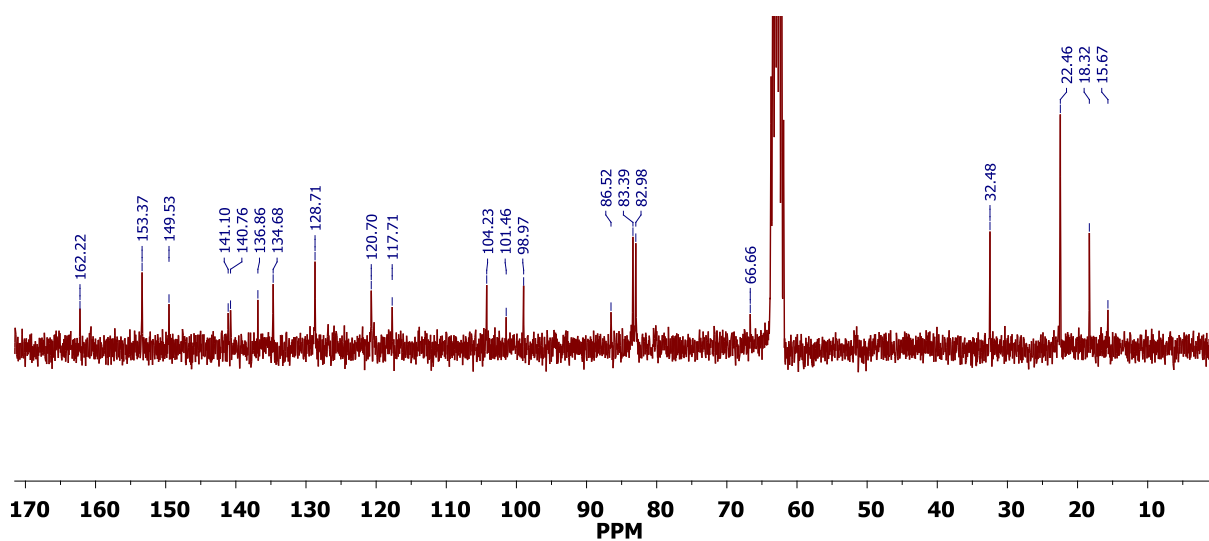


**Figure S4.**  $^{13}\text{C}$  NMR of complex **3** in Nitromethane- $\text{d}_3$

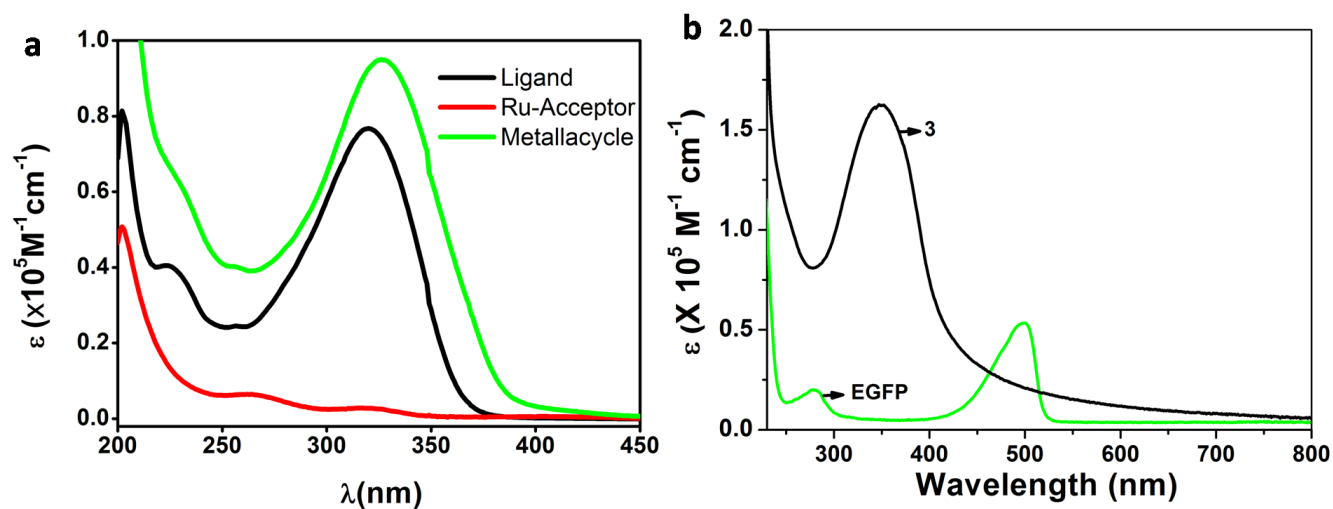


**Figure S5.** (a) Electronic absorption spectrum of ligand **1** (black), diruthenium precursor **2** (red), and [2 + 2] self-assembly **3** (green) collected from  $1 \times 10^{-5}$  M solutions in MeOH. (b) Electronic absorption spectrum of EGFP ( $2 \times 10^{-6}$  M), TCMC **3** (20  $\mu\text{M}$ ) in 10 mM Tris HCl solution pH 7.0 .

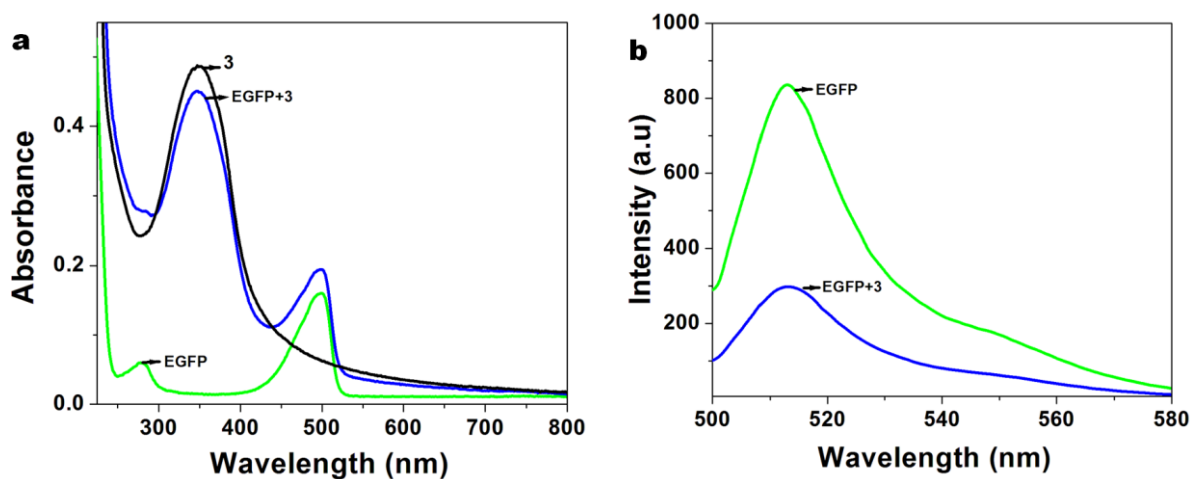


**Figure S6.** (a) UV/vis absorption spectra of EGFP ( $2 \times 10^{-6}$  M), **3** (20  $\mu\text{M}$ ) and EGFP + **3** in 10 mM Tris HCl solution (left). (b) Emission spectra of EGFP ( $2 \times 10^{-6}$  M) and EGFP + **3** (right).

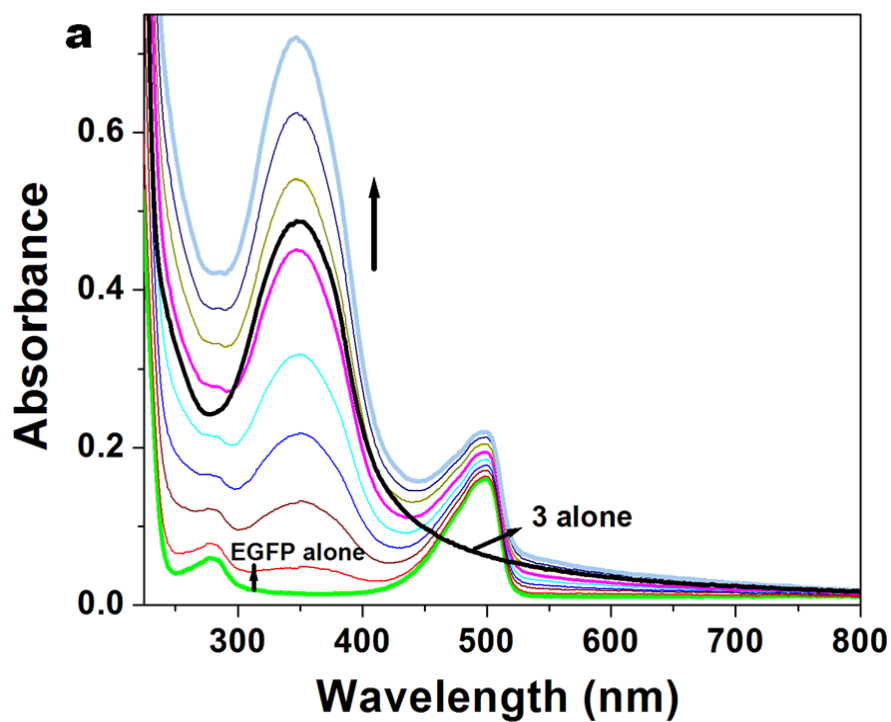


**Figure S7.** UV/vis absorption spectra of EGFP ( $2 \times 10^{-6}$  M) upon incremental addition of **3** (0-32  $\mu$ M (left). Arrows show the absorbance changes upon increasing the amount of **3**.

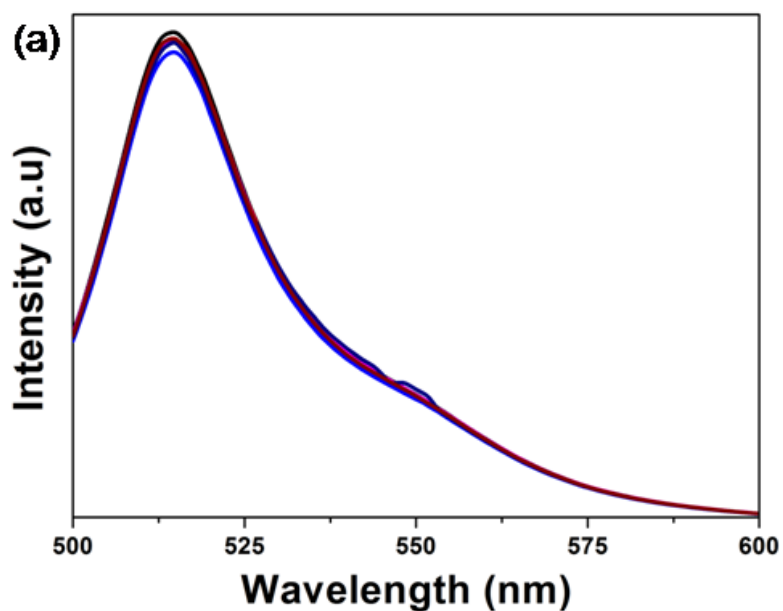


**Figure S8.** Emission spectra of EGFP ( $2 \times 10^{-6}$  M) upon addition of **4** (0-20  $\mu$ M)

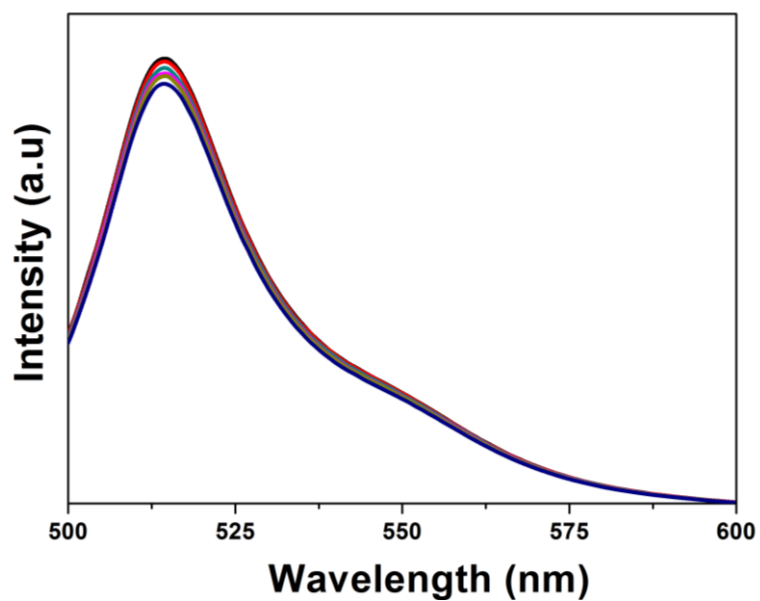


**Figure S9.** Emission spectra of EGFP ( $2 \times 10^{-6}$  M) upon addition of **5** (0-20 μM)

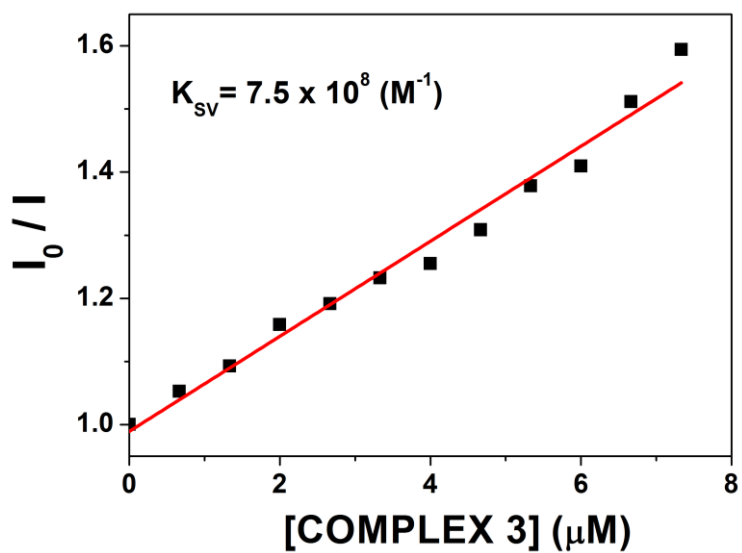


**Figure S10.** Stern–Volmer plots for the interaction of **3** with EGFP fitting a plot of ( $I_0/I$ ) versus [ $C_3$ ], C-Concentration of complex **3**.

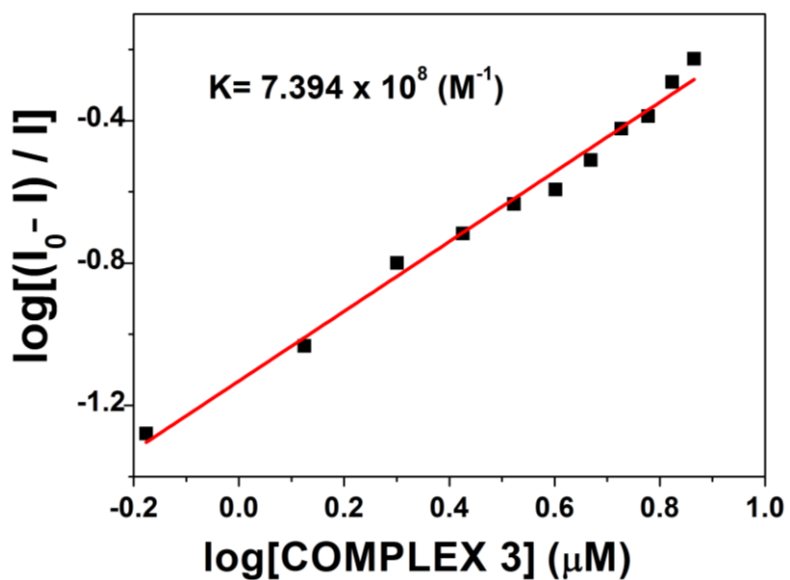


**Figure S11.** Plots for the interaction of **3** with EGFP fitting a plot of  $\log(I_0 - I / I)$  versus  $\log[\text{Complex } 3]$ .

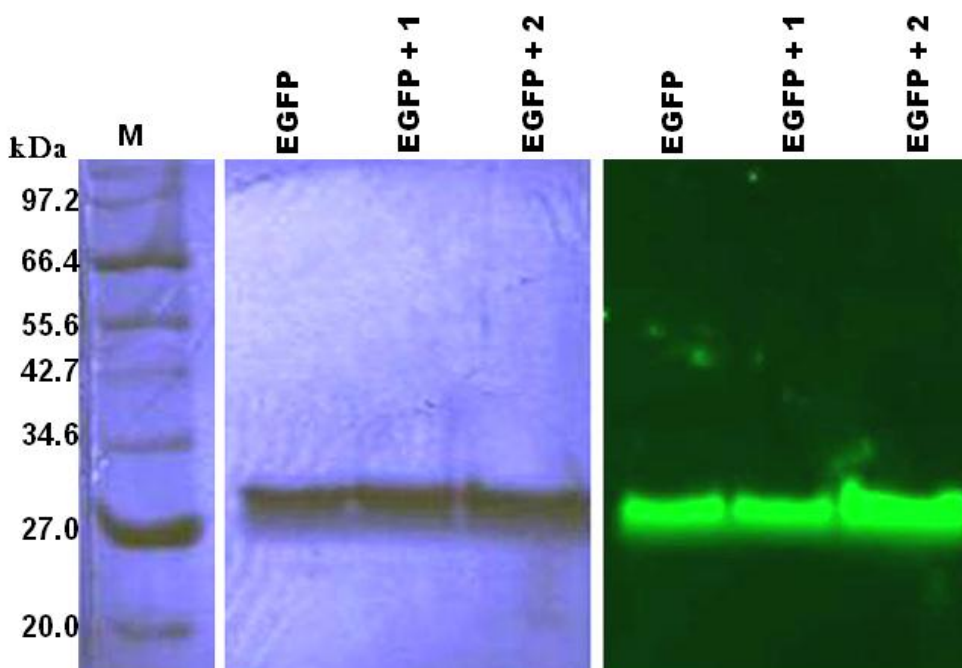


**Figure S12.** SDS-PAGE of EGFP (5  $\mu\text{M}$ ) incubated at 37°C with **1** and **2** (10  $\mu\text{M}$ ) in a 5% DMSO/10mM Tris-HCl buffer (pH 7.0). Gel exposed to Coomassie stain (*left*) and UV light (*right*).

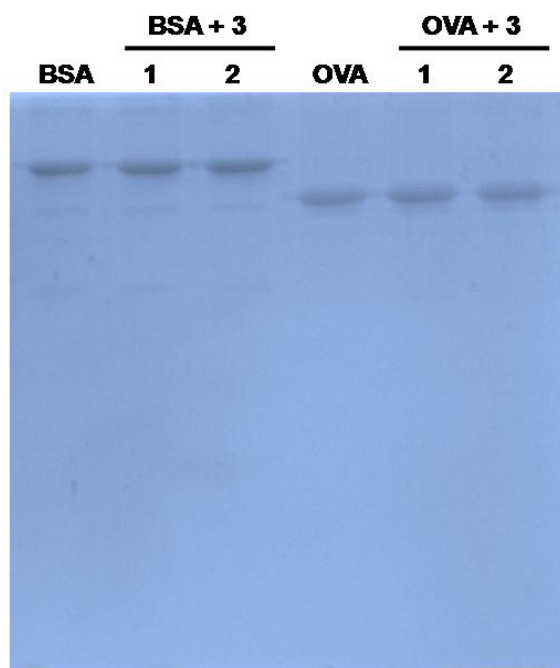


**Figure S13.** SDS-PAGE of BSA (2  $\mu$ M) and OVA (2  $\mu$ M) incubated at 37°C for 60 min with **3** in a 5% DMSO/10mM Tris-HCl buffer (pH 7.0). Protein incubated with 2  $\mu$ M (1), 10  $\mu$ M (2).

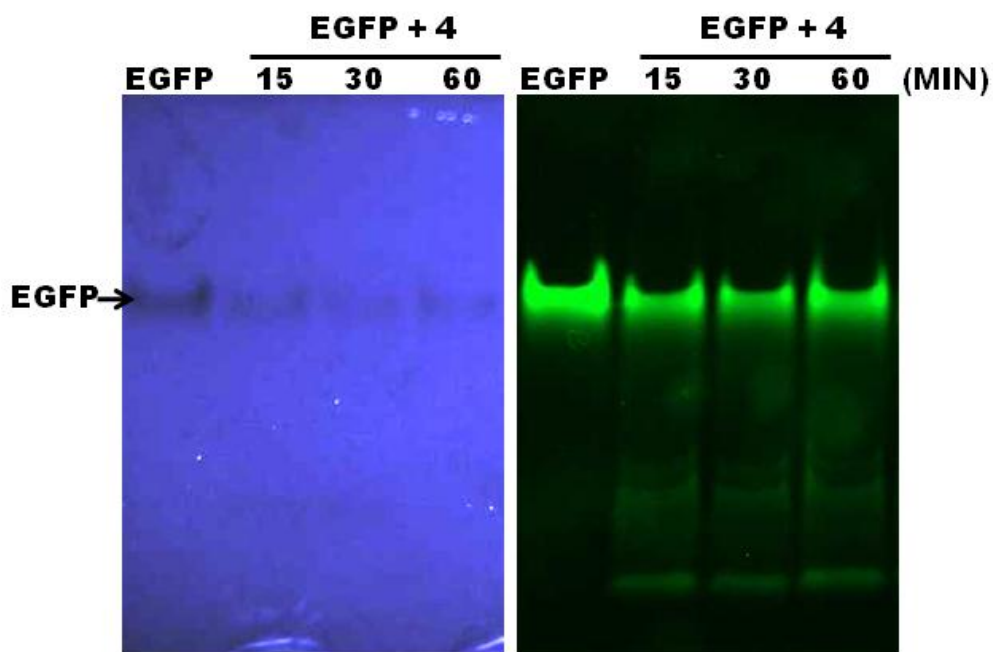


**Figure S14.** SDS-PAGE of EGFP (5  $\mu$ M) incubated at 37 °C with **4** (10  $\mu$ M) in a 5% DMSO/10mM Tris-HCl buffer (pH = 7.0) exposed to Coomassie blue stain (*left*) and UV light (*right*).

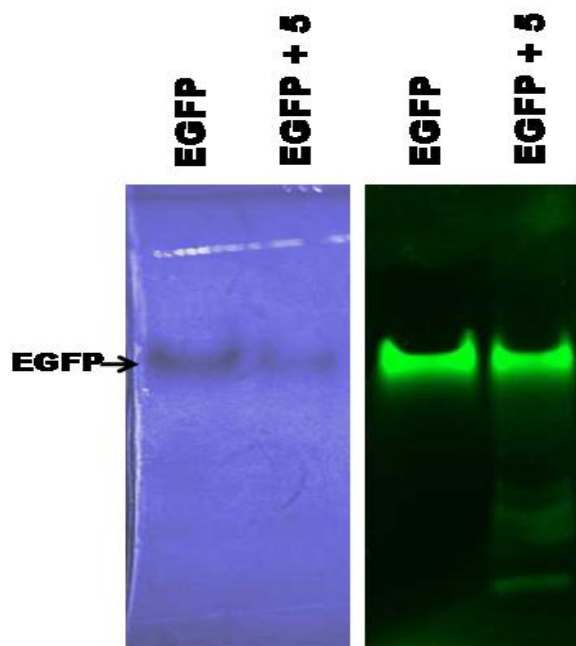


**Figure S15.** SDS-PAGE of EGFP (5  $\mu\text{M}$ ) incubated at 37  $^{\circ}\text{C}$  for 60 min with **5** (10  $\mu\text{M}$ ) in a 5% DMSO/10mM Tris-HCl buffer (pH = 7.0) exposed to Coomassie blue stain (*left*) and UV light (*right*).

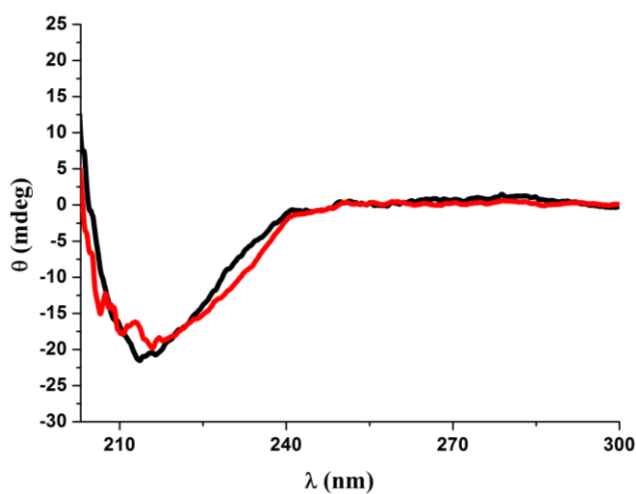


**Figure S16.** Circular dichroism spectrum of 11.2  $\mu\text{M}$  EGFP in the presence of **5** (8.3  $\mu\text{M}$ ) in 10 mM Tris HCl buffer, pH 7.0.

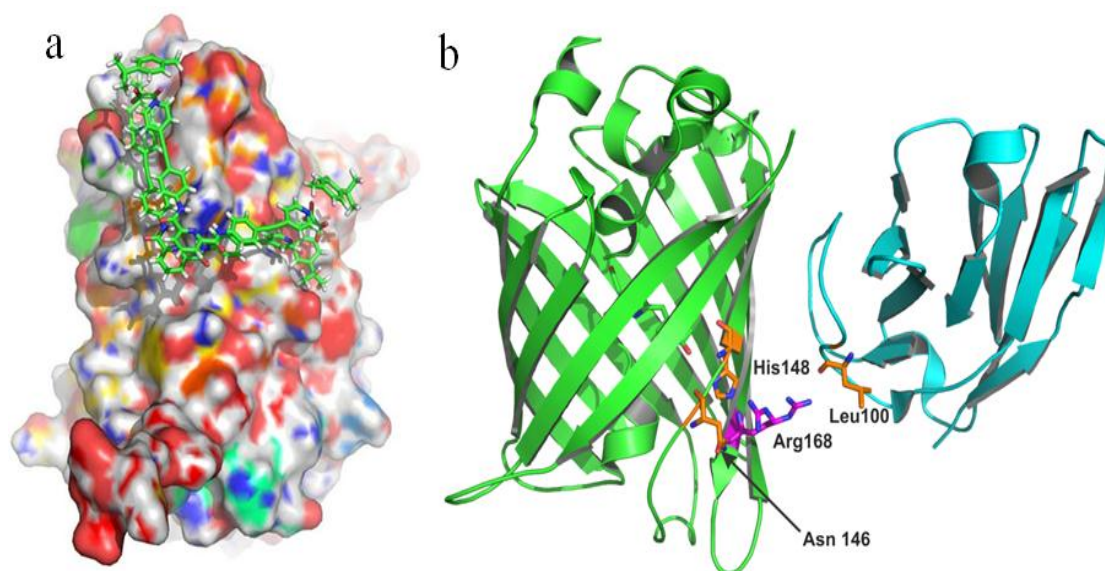


**Figure S17:** (a) Surface representation of the EGFP protein interacting with SCC 3. (b) Structural conformation of minimizer (Cyan colored ribbon) bound EGFP (Green colored ribbon) showing two different conformation for Arg168 (Highlighted in pink colored sticks). One conformation of Arg168 interacts with the Leu 100 and loses its interaction with His 148 and Asn 146. Other conformation of Arg168 interacts with Asn146 and His 148. (PDB ID of the minimizer bound GFP – 3G9A)

**Table S1:** PDBID, query coverage and identity of the 3D structural templates of EGFP obtained through Blastp (Co-crystallized with nanobody) for our EGFP variant.

PDBID	Nanobody	Query coverage Of protein sequence	Sequence Identity
1GFL	-	89%	98%
3OGO <sup>[17]</sup>	Enhancer	89%	99%
3G9A <sup>[18]</sup>	Minimizer	89%	97%
3K1K <sup>[18]</sup>	Enhancer	89%	96%

Structural comparison of the enhancer/minimizer bound EGFP shows that the two different conformation of EGFP. From the comparison between the 3K1K and 3G9A structures,<sup>1</sup> it is clear that Arg168 adopts a

two different conformation, as shown in figure S6. Using 3K1K and 3G9A, two model structures were optimized for our EGFP variant by using modeler software. Before constructing the model, a sequence alignment was performed using ClustalX<sup>2</sup> and was compared with the align2D tool of modeler and manually checked. The overall stereochemical and structural qualities of the constructed model protein was assessed using SAVES server.<sup>3</sup>

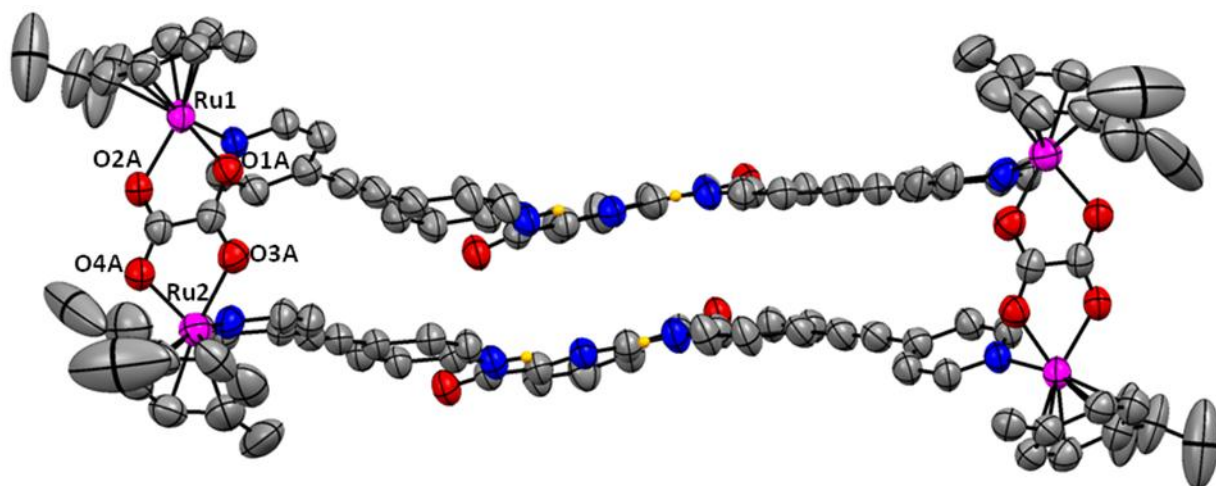


**Figure S18.** Molecular structure of complex **3** (thermal ellipsoids are drawn at 50% probability; only amidic hydrogen atoms are shown for clarity)

**Table S2.** Crystal data and structure refinement for **3**.

Empirical formula	C127 H153 F12 N10 O29 Ru4 S4	
Formula weight	3044.11	
Temperature	100(2) K	
Wavelength	0.80000 Å	
Crystal system	Monoclinic	
Space group	<i>C2/c</i>	
Unit cell dimensions	$a = 32.701(7)$ Å	$\alpha = 90^\circ$
	$b = 18.016(4)$ Å	$\beta = 114.20(3)^\circ$
	$c = 23.371(5)$ Å	$\gamma = 90^\circ$
Volume	$12559(5)$ Å <sup>3</sup>	
Z	4	
Density (calculated)	1.610 g/cm <sup>3</sup>	
Absorption coefficient	0.863 mm <sup>-1</sup>	
F(000)	6260	
Crystal size	$0.25 \times 0.25 \times 0.20$ mm <sup>3</sup>	
Theta range for data collection	1.49 to 30.36°	
Index ranges	$-39 \leq h \leq 40, -21 \leq k \leq 21, -26 \leq l \leq 27$	
Reflections collected	36226	
Independent reflections	10243 [R(int) = 0.0294]	
Completeness to theta = 27.50°	96.5 %	

Absorption correction	Semi-empirical from equivalents
Max. and min. transmission	0.8464 and 0.8132
Refinement method	Full-matrix least-squares on F <sup>2</sup>
Data / restraints / parameters	10243 / 116 / 845
Goodness-of-fit on F <sup>2</sup>	1.300
Final R indices [I > 2σ(I)]	R1 = 0.0907, wR2 = 0.2811
R indices (all data)	R1 = 0.1032, wR2 = 0.2939
Extinction coefficient	0.0038(4)
Largest diff. peak and hole	1.688 and -1.102 e.Å <sup>-3</sup>

**Table S3.** Selected Bond lengths [Å] and angles [°] for **3**.

---

Ru(1)-O(2A)	2.115(4)
Ru(1)-N(1C)	2.114(5)
Ru(1)-O(1A)	2.141(5)
Ru(2)-N(5C)#1	2.085(6)
Ru(2)-O(3A)	2.113(5)
Ru(2)-O(4A)	2.118(5)
N(5C)-Ru(2)#1	2.085(6)
O(2A)-Ru(1)-N(1C)	87.81(17)
O(2A)-Ru(1)-O(1A)	78.11(16)
N(1C)-Ru(1)-O(1A)	81.63(18)
N(5C)#1-Ru(2)-O(3A)	85.36(19)
N(5C)#1-Ru(2)-O(4A)	82.51(19)
O(3A)-Ru(2)-O(4A)	78.83(17)
C(32C)-N(5C)-Ru(2)#1	122.8(4)
C(33C)-N(5C)-Ru(2)#1	119.9(4)

---

Symmetry transformations used to generate equivalent atoms:

#1 -x,y,-z+1/2

**References:**

1. A. Kirchhofer, J. Helma, K. Schmidthals, C. Frauer, S. Cui, A. Karcher, M. Pellis, S. Muyltermans, C. S. Casas-Delucchi, M. C. Cardoso, H. Leonhardt, K. P. Hopfner and U. Rothbauer, *Nat. Struct. Mol. Biol.*, 2009, **17**, 133.

2. M. A. Larkin, G. Blackshields, N. P. Brown, R. Chenna, P. A. McGettigan, H. McWilliam, F. Valentin, I. M. Wallace, A. Wilm, R. Lopez, J. D. Thompson, T. J. Gibson and D. G. Higgins, *Bioinformatics*, 2007, **23**, 2947.
3. R. A. Laskowski, M. W. MacArthur, D. S. Moss and J. M. Thornton, *Journal of Applied Crystallography*, 1993, **26**, 283.